Processivity and collectivity of biomolecular motors extracting membrane nanotubes

DOI:
10.1103/PhysRevE.86.010901

Document status and date:
Published: 01/01/2012

Document Version:
Publisher's PDF, also known as Version of Record (includes final page, issue and volume numbers)

PHYSICAL REVIEW E **86**, 010901(R) (2012)

Processivity and collectivity of biomolecular motors extracting membrane nanotubes

Francisco Fontenele Araujo and Cornelis Storm
Department of Physics and Institute for Complex Molecular Systems, Eindhoven University of Technology, P.O. Box 513, 5600 MB Eindhoven, The Netherlands

(Received 6 February 2012; published 23 July 2012)

Biomolecular motors can pull and viscously drag membranes. The resulting elongations include cell protrusions, tether networks, and sensorial tentacles. Here we focus on the extraction of a single tube from a vesicle. Via a force balance coupled to binding kinetics, we analytically determine the phase diagram of tube formation as function of the motor processivity, the surface viscosity of the membrane η'_m, and the density of motors on the vesicle ρ. Three tubulation mechanisms are identified: (i) tip pulling, due to the accumulation of motors at the leading edge of the membrane, (ii) viscous drag, emergent from the translation of motors along the tube, and (iii) hybrid extraction, such that tip pulling and viscous drag are equally important. For experimental values of η'_m and ρ, we find that the growth of bionanotubes tends to be driven by viscous forces, whereas artificial membranes are dominated by tip pulling.

DOI: 10.1103/PhysRevE.86.010901 PACS number(s): 87.16.Nn, 87.16.D−

Membranes are fluid-lipid interfaces of remarkable biological functionality. They mediate transport processes at the cellular level, exhibiting soft mechanical properties and highly adaptive geometries. Vesicles, for instance, hold a spherical shape under most equilibrium conditions. But in the presence of spatiotemporal stimuli, membrane tubes can emerge over lengths of several micrometers with diameters in the nanometer scale [1,2]. This is the case of sensorial tentacles developed during phagocytosis [3] and intercellular tethers activated by the transmission of viruses [4]. *In vitro* experiments mimicking such vesicotubular structures have been performed via micropipette aspiration [5], optical tweezers [6], polymerization of biofilaments [7], concentration gradients [8], and molecular motors [9–15]. The latter scenario, in particular, is sketched in Fig. 1.

The force necessary to extract a membrane tube is typically five times larger than the pulling scale $f_0 \simeq 5$ pN associated with a single motor protein [9–15]. Overcoming this barrier requires at least two physical conditions: (i) a sufficiently high density of motors on the vesicle and (ii) a sustainable kinetics of motor binding to the substrate. Furthermore, the mechanical work done by each bound motor depends on its processivity. Kinesin, for example, can walk hundreds of steps before unbinding from the substrate. Nonclaret disjunctional (Ncd) proteins, on the other hand, detach just after a couple of steps. According to fluorescence imaging experiments [9], Ncd motors spread out along the tube, while kinesins cluster at the tip.

From the theoretical standpoint, the picture of tip clustering has been extensively studied in terms of stochastically interacting particles [10,11,13,16,17], deterministic dynamical systems [12], and mean field equations [14]. Nevertheless, the models proposed so far have not considered how the tubulation phenomenon depends on the processivity of the motors and on the surface viscosity η'_m of the membrane. Both aspects are relevant, since nonprocessive motors execute key tasks at cellular level and biological membranes may be significantly more viscous than artificial ones. Phosphatidylcholine (PC) membranes, for instance, have $\eta'_m \simeq 10^{-10}$–10^{-9} Pa m s [18,19], whereas values as high as $\eta'_m \simeq 10^{-4}$ Pa m s are reported for red blood cells [20,21]. This fact, together with the lack of comparable differences in the bending rigidity $\kappa_c \simeq 10^{-20}$–10^{-19} J [21–23] and in the stretching modulus $\kappa_{\mathrm{A}} \simeq 0.1$–$1$ N/m [22,23], raises questions about the role of η'_m in motor-membrane interactions. In particular, what is the impact of η'_m on the driving force behind tube formation? Can η'_m affect the spatial distribution of motors along the tube? And what is the interplay between viscous and (non)processivity effects? The present Rapid Communication addresses these issues via a simple force balance coupled to the binding kinetics of motors.

Model setup. As shown in Fig. 1, consider a spherical vesicle of radius R immersed in an fluid of viscosity η_w. The vesicle is coated with a density ρ of molecular motors, which bind and unbind to the substrate at constant rates k_b and k_u, respectively. While bound, each motor takes unidirectional steps of length ℓ, exerting a force on the membrane. This induces the formation of a tube, which we define as a cylinder of length L capped by a hemisphere of radius $r = \sqrt{\kappa_c/(2\sigma)}$ [1,2].

Tube growth evolves slower than the speed v_0 of a free molecular motor. Typically, $\dot{L} \simeq 0.15 v_0$ [9,14], suggesting that the population of bound motors experiences a velocity drop along the axial length L. A convenient way to approach this effect consists in decomposing the tube into two parts: stem and tip [12,13], as illustrated in Fig. 2. The tip is formed by n_b bound motors that walk at the same speed $\dot{L}$ of the tube, pulling the membrane with a force f_b. The remaining N_b bound motors have a velocity surplus $v_0 - \dot{L}$ that defines the stem. Their viscous drag force on the membrane is F_b.

Stem force. In the course of their walk on the substrate, stem motors impart momentum to the membrane tube. The corresponding force can be expressed as $F_b \equiv N_b F_\zeta$, where $F_\zeta \equiv \zeta(v_0 - \dot{L})$ denotes the viscous drag of a single motor on the membrane. The coefficient ζ is nontrivial, because it involves the following: (i) the size λ of the protein domain moving in the membrane and (ii) the local radius of curvature r of the membrane relative to the Saffman-Delbrück length $\ell_\eta \equiv \eta'_m/\eta_w$ (the scale below which η'_m dominates the viscous dissipation [24]). According to recent experiments [25] and theoretical analyses [24,26], the axial drag coefficient in a

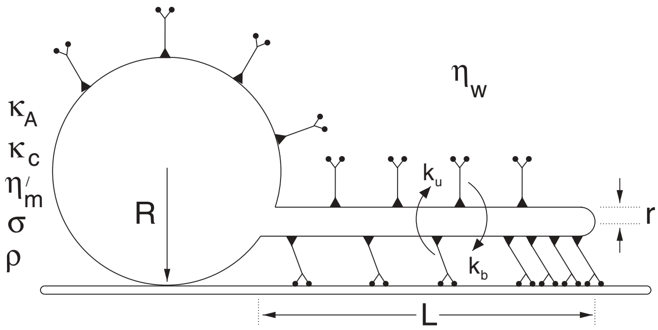

FIG. 1. Sketch of membrane tubulation by molecular motors. The vesicle has radius R, stretching modulus κ_A, bending rigidity κ_c, surface viscosity η'_m, and surface tension σ. Molecular motors are attached to the membrane by their tails (triangles), so that the surface density on the vesicle is ρ. Motor heads (circles) are free to bind and unbind to the substrate at rates k_b and k_u, respectively. While bound, each motor takes unidirectional steps of length ℓ, exerting a force on the membrane. The tube has length L and radius $r = \sqrt{\kappa_c/(2\sigma)}$. The viscosity of the aqueous surrounding is η_w.

cylindrical membrane of radius $r \ll \ell_\eta$ is given by [24]

$$\zeta = \frac{4\pi\eta'_m}{\ln(r/\lambda) + \frac{1}{2}}. \tag{1}$$

In the context of this Rapid Communication, we take $r = \sqrt{\kappa_c/(2\sigma)}$ and identify the length λ with the tail of the molecular motor. The resulting stem force,

$$F_b = N_b \frac{4\pi\eta'_m(v_0 - \dot{L})}{\ln(r/\lambda) + \frac{1}{2}}, \tag{2}$$

is to be compared with its counterpart f_b at the tip.

Tip force. Towards the hemispherical cap of the tube, the membrane exhibits a curvature change around which n_b bound motors have their velocities reduced to $\dot{L}$. Such a drop depends on the force-velocity properties of the molecular motors. In its simplest form, the force f_1 due to a single motor is given by $f_1 = f_0(1 - v/v_0)$, where f_0 denotes the stall force and v the motor velocity under load [27]. On the basis of this individual contribution, we write the force $f_b \equiv n_b f_1(\dot{L})$ on the tip of the tube as

$$f_b = n_b f_0 \left(1 - \frac{\dot{L}}{v_0}\right). \tag{3}$$

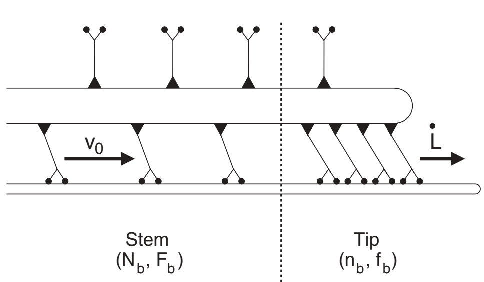

FIG. 2. Stem-tip decomposition. Tip: Set of n_b bound motors that walk at speed $\dot{L}$, pulling the membrane with a force f_b. Stem: Population of N_b bound motors with velocity surplus $v_0 - \dot{L}$, which viscously drag the membrane with a force F_b. The collective force due to stem and tip motors is $\mathcal{F}_b = F_b + f_b$.

Multimotor force versus membrane force. The multimotor drive $\mathcal{F}_b = F_b + f_b$ is opposed by the membrane force $\mathcal{F}_m$. But how does $\mathcal{F}_m$ depend on the mechanical and geometrical properties of the vesicotubular structure? We assume $\mathcal{F}_m = \mathcal{F}_c + \mathcal{F}_A$, such that $\mathcal{F}_c = 2\pi\sqrt{2\sigma\kappa_c}$ is the barrier for tube formation [1,2] and $\mathcal{F}_A$ the stretching force. The latter arises from the energy $\mathcal{E}_A \equiv \kappa_A(A - A_0)^2/(2A_0)$, where A_0 and A are the areas of the unstretched and stretched membranes, respectively [1]. For tube extraction from a spherical vesicle, $A_0 = 4\pi R^2$, $A - A_0 \approx 2\pi r L$, and $\mathcal{E}_A = \frac{1}{2}\kappa_A\pi\,(r/R)^2\,L^2$. Thus, $\mathcal{F}_A \equiv \partial\mathcal{E}_A/\partial L = \kappa_A\pi\,(r/R)^2\,L$, leading to

$$\mathcal{F}_m = 2\pi\sqrt{2\sigma\kappa_c} + \kappa_A\pi\left(\frac{r}{R}\right)^2 L. \tag{4}$$

Balancing $\mathcal{F}_b$ and $\mathcal{F}_m$, one readily finds

$$\frac{v_0 - \dot{L}}{v_0} = \frac{2\pi\sqrt{2\sigma\kappa_c} + \kappa_A\pi\,(r/R)^2\,L}{N_b\zeta v_0 + n_b f_0}. \tag{5}$$

Equation (5) governs the evolution of the tube length L and the current $J_b \equiv (v_0 - \dot{L})N_b/L$ of bound motors towards the tip [12]. Both are coupled to the binding kinetics.

Binding kinetics. The membrane tube hosts a total of $\mathcal{N} = 2\pi r L\rho$ motors, of which $\mathcal{N}_b = N_b + n_b$ bound and $\mathcal{N}_u = \mathcal{N} - \mathcal{N}_b$ unbound to the substrate. We model the binding kinetics over the stem and tip regions by

$$\frac{dN_b}{dt} = I - k_u N_b - J_b, \tag{6}$$

$$\frac{dn_b}{dt} = J_b - k_u n_b, \tag{7}$$

where I denotes the influx of motors to the filament. This flux involves geometric constraints and excluded volume effects on binding. We assume $I = k_b\mathcal{N}_a(1 - \phi_b)$, where $\mathcal{N}_a$ is the number of attachable motors and ϕ_b the occupation of the filament. Letting $\mathcal{N}_\parallel$ denote the number of tracks accessible to a motor (see Fig. 3 and Ref. [13]), we estimate the number of stepping sites as $\mathcal{N}_\parallel L/\ell$ and $\phi_b \simeq (N_b + n_b)/(\mathcal{N}_\parallel L/\ell)$. Analogous arguments hold for $\mathcal{N}_a$. Considering that unbound motors tend to be uniformly distributed on the membrane, only those on the lower surface of the tube can bind to a track. The corresponding fraction of attachable motors is ϕ_a

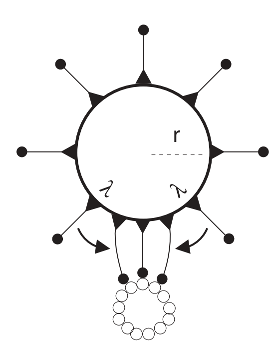

FIG. 3. Sketch of a cross section of the membrane tube [13]. The number of accessible tracks for motor binding depends on the relative proportions between tube, motors, and filament. Among the unbound motors, only those neighboring the filament are attachable. For kinesins walking on a microtubule, $\mathcal{N}_\parallel \simeq 3$ protofilaments [13] and the motor tail $\lambda \simeq 20$ nm [28].

so that $\mathcal{N}_a = \phi_a \mathcal{N}_u$. As shown in Fig. 3, $\phi_a \simeq (2\lambda)/(2\pi r)$ since a cross section of the tube hosts two unbound motors that neighbor the filament. In terms of such estimates, $I = k_b \frac{\lambda}{\pi r}(2\pi r L\rho - N_b - n_b)(1 - \frac{N_b+n_b}{\mathcal{N}_\parallel L/\ell})$.

Dimensionless equations. Introducing $\tau \equiv t k_u$ and $X \equiv L/\ell$, Eqs. (5)–(7) can be written in dimensionless form as

$$\frac{dX}{d\tau} = P\left(1 - \frac{E+SX}{N_b D + n_b}\right), \tag{8}$$

$$\frac{dN_b}{d\tau} = B\phi_a (MX - N_b - n_b)\left(1 - \frac{N_b+n_b}{\mathcal{N}_\parallel X}\right) - N_b - \frac{PN_b}{X}\left(\frac{E+SX}{N_b D + n_b}\right), \tag{9}$$

$$\frac{dn_b}{d\tau} = \frac{PN_b}{X}\left(\frac{E+SX}{N_b D + n_b}\right) - n_b, \tag{10}$$

where $P \equiv v_0/(\ell k_u)$, $E \equiv 2\pi\sqrt{2\sigma\kappa_c}/f_0$, $S \equiv \kappa_A \pi (r/R)^2 \ell/f_0$, $D \equiv \zeta v_0/f_0$, $B \equiv k_b/k_u$, and $M \equiv 2\pi r \ell \rho$. These dimensionless parameters comprise one indicator of collectivity (number M of motors in a tube element of radius r and length ℓ), two kinetic ratios (representing binding B and processivity P), and three force ratios (extraction barrier E, viscous drag D, and membrane stretching S). In terms of them, the dimensionless current $j_b \equiv J_b/k_u$ is given by $j_b = P(N_b/X)(E+SX)/(N_b D + n_b)$.

Collectivity and processivity. Focus on motor collectivity and processivity suggests the study of Eqs. (8)–(10) as a function of M and P. The former is experimentally controllable via the density ρ of motors on the vesicle. The latter involves stepping and unbinding properties, in such a way that $P = 1$ for an ideal nonprocessive motor and $P \gg 1$ for processive motors. Of particular interest is the question of how M and P are reflected in the driving force of tube extraction. To address this issue, we consider the ratio $F_b/f_b = DN_b/n_b$, where $D = 4\pi\eta'_m v_0 f_0^{-1}/[\ln(r/\lambda) + \frac{1}{2}]$. Depending on the surface viscosity η'_m of the membrane, three tubulation mechanisms can emerge: (i) tip pulling, where $f_b > F_b$, (ii) viscous drag, for which $F_b > f_b$, and (iii) hybrid extraction, such that $F_b = f_b$. Since hybrid extraction is a key limiting case, we shall determine its steady state solution $(\overline{X}, \overline{N}_b, \overline{n}_b)$ and its locus on the $\eta'_m \times \rho$ plane.

Steady state and phase diagram. Setting $d\overline{X}/d\tau = d\overline{N}_b/d\tau = d\overline{n}_b/d\tau = 0$ in Eqs. (8)–(10) and invoking the condition $\overline{F_b} = \overline{f_b}$, one analytically finds

$$\overline{X} = \frac{P}{D}, \quad \overline{N}_b = \frac{E}{2D} + \frac{PS}{2D^2}, \quad \overline{n}_b = \frac{E}{2} + \frac{PS}{2D}. \tag{11}$$

This leads to a current $\overline{j_b} = \overline{n}_b \sim P/D$ that linearly increases with processivity and monotonically decreases with the membrane viscosity. The corresponding density of motors, though, has a more involved dependence on P and D. It follows from Eq. (9) evaluated at (11),

$$\overline{M} = \frac{\left(\frac{1}{B\phi_a} + 1 - \overline{\phi_b}\right)\mathcal{N}_\parallel \overline{\phi_b}}{1 - \overline{\phi_b}}, \tag{12}$$

with $\overline{\phi_b} \equiv (\overline{N}_b + \overline{n}_b)/(\mathcal{N}_\parallel \overline{X})$. Here, the tube length $\overline{X}$ and the number of stepping tracks $\mathcal{N}_\parallel$ limit the population of bound motors $\overline{N}_b + \overline{n}_b$, so that Eq. (12) is physically relevant only if

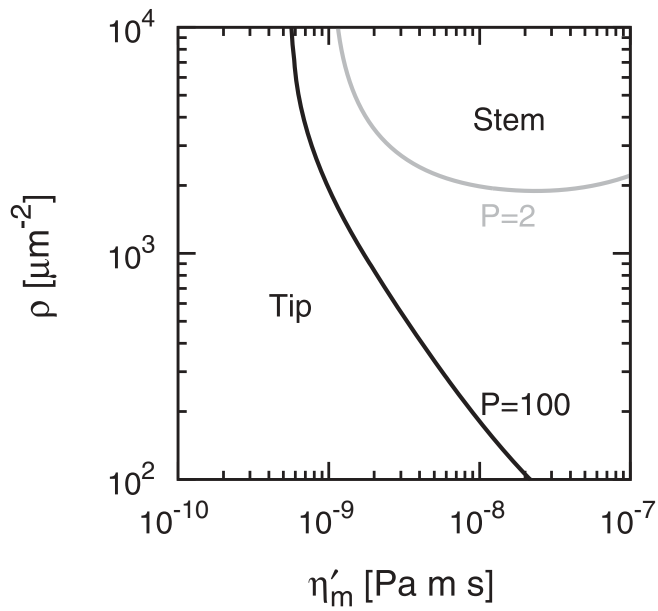

FIG. 4. Phase diagram of membrane tubulation by molecular motors. Abscissa: Surface viscosity of the membrane η'_m. Ordinate: Density ρ of motors on the vesicle. Gray line: Hybrid extraction for $P = 2$ (nonprocessive motors). Black line: Asymptotic boundary between tip pulling and stem drag for $P \gtrsim 100$ (processive motors). Here, P is changed via the unbinding rate k_u, while keeping $B = 10$. The remaining parameters are fixed at typical experimental values: $R = 10\ \mu$m, $\sigma = 10^{-4}$ N/m, $\kappa_A = 0.2$ N/m, $\kappa_c = 10^{-19}$ J, $f_0 = 5$ pN, $\ell = 10$ nm, $\lambda = 20$ nm, $v_0 = 500$ nm/s, and $\mathcal{N}_\parallel = 3$.

$\overline{\phi_b} < 1$. This constraint is violated at membrane viscosities (e.g., $\eta'_m \lesssim 10^{-9}$ Pa m s) for which $\overline{F_b} = \overline{f_b}$ requires an excessive number of bound motors. Discarding $\overline{\phi_b} \geqslant 1$ from the graphical representation of Eq. (12), we plot in Fig. 4 the hybrid extraction density as function of the membrane viscosity, for motors at low ($P = 2$) and at high ($P = 100$) processivities.

Discussion. What are the biophysical implications of Fig. 4? On the one hand, we note that the experiments of Refs. [9–15] remarkably fall into the viscosity range $\eta'_m \simeq 10^{-10}$–10^{-9} Pa m s. This is within the dominance of the tip force, because of the artificiality of PC membranes rather than the processivity of the motors. In contrast, biological membranes are more viscous ($\eta'_m \gtrsim 10^{-8}$ Pa m s [20,21]) and hence susceptible to the drag exerted by stem motors. For instance, tubulation in a neuron ($\eta'_m \simeq 10^{-8}$ Pa m s [20]) by kinesins ($P \simeq 100$ at, say, $\rho = 500\ \mu m^{-2}$) falls into the stem regime. But as the processivity is decreased from $P = 100$ to $P = 2$, the hybrid extraction line is shifted to higher densities so that $\rho \gtrsim 10^3\ \mu m^{-2}$. Physically, this degree of motor collectivity seems indeed required to compensate large membrane viscosities.

Summary and outlook. On the basis of forces (2)–(4) and binding kinetics (6) and (7), we sketched the phase diagram of membrane tubulation by molecular motors. Our results of Fig. 4 indicate that artificial (PC) membranes inexorably fall into the tip regime, whereas biological membranes can be dragged by stem motors. Such a contrast suggests that the surface viscosity η'_m likely affects the spatial distribution of bound motors. In particular, since the current $J_b \sim 1/\eta'_m$, we expect that the accumulation of processive motors at the tip of nanotubes becomes less pronounced for increasing η'_m. Fluorescence imaging experiments could tackle this issue, along the lines of Ref. [9].

Acknowledgments. This work is supported by NanoNextNL, a micro and nanotechnology program of the Dutch Ministry of Economic Affairs, Agriculture & Innovation (EL&I), and 130 partners.

[1] R. Phillips, J. Kondev, and J. Theriot, *Physical Biology of the Cell* (Garland Science, New York, 2008).
[2] I. Derényi, F. Jülicher, and J. Prost, Phys. Rev. Lett. **88**, 238101 (2002).
[3] P. K. Mattila and P. Lappalainen, Nat. Rev. Mol. Cell Biol. **9**, 446 (2008).
[4] D. M. Davis and S. Sowinski, Nat. Rev. Mol. Cell Biol. **9**, 431 (2008).
[5] E. Evans, H. Bowman, A. Leung, D. Needham, and D. Tirrell, Science **273**, 933 (1996).
[6] G. Koster, A. Cacciuto, I. Derenyi, D. Frenkel, and M. Dogterom, Phys. Rev. Lett. **94**, 068101 (2005).
[7] A. P. Liu, D. Richmond, L. Maibaum, S. Pronk, P. L. Geissler, and D. A. Fletcher, Nat. Phys. **4**, 789 (2008).
[8] F. Campelo and A. Hernández-Machado, Phys. Rev. Lett. **100**, 158103 (2008).
[9] P. M. Shaklee, L. Bourel-Bonnet, M. Dogterom, and T. Schmidt, Biophys. J. **98**, 93 (2010).
[10] P. M. Shaklee, T. Idema, L. Bourel-Bonnet, M. Dogterom, and T. Schmidt, Biophys. J. **99**, 1835 (2010).
[11] P. M. Shaklee, T. Idema, G. Koster, C. Storm, T. Schmidt, and M. Dogterom, Proc. Natl. Acad. Sci. USA **105**, 7993 (2008).
[12] O. Campàs, C. Leduc, P. Bassereau, J. F. Joanny, and J. Prost, Biophys. Rev. Lett. **4**, 163 (2009).
[13] O. Campàs, C. Leduc, P. Bassereau, J. Casademunt, J. F. Joanny, and J. Prost, Biophys. J. **94**, 5009 (2008).
[14] C. Leduc, O. Campàs, K. B. Zeldovich, A. Roux, P. Jolimaitre, L. Bourel-Bonnet, B. Goud, J. F. Joanny, P. Bassereau, and J. Prost, Proc. Natl. Acad. Sci. USA **101**, 17096 (2004).
[15] G. Koster, M. van Duijn, and M. Dogterom, Proc. Natl. Acad. Sci. USA **100**, 15583 (2003).
[16] J. Tailleur, M. R. Evans, and Y. Kafri, Phys. Rev. Lett. **102**, 118109 (2009).
[17] O. Campàs, Y. Kafri, K. B. Zeldovich, J. Casademunt, and J. F. Joanny, Phys. Rev. Lett. **97**, 038101 (2006).
[18] W. K. den Otter and S. A. Shkulipa, Biophys. J. **93**, 423 (2007).
[19] R. Dimova, S. Aranda, N. Bezlyepkina, V. Nikolov, K. A. Riske, and R. Lipowsky, J. Phys.: Condens. Matter **18**, S1151 (2006).
[20] F. Brochard-Wyart, N. Borghi, and P. Nassoy, Proc. Natl. Acad. Sci. USA **103**, 7660 (2006).
[21] R. M. Hochmuth and W. D. Marcus, Biophys. J. **82**, 2964 (2002).
[22] W. Rawicz, K. C. Olbrich, T. McIntosh, D. Needham, and E. Evans, Biophys. J. **79**, 328 (2000).
[23] E. Evans and W. Rawicz, Phys. Rev. Lett. **64**, 2094 (1990).
[24] M. L. Henle and A. J. Levine, Phys. Rev. E **81**, 011905 (2010).
[25] Y. A. Domanov, S. Aimon, G. E. S. Toombes, M. Renner, F. Quemeneur, A. Triller, M. S. Turner, and P. Bassereau, Proc. Natl. Acad. Sci. USA **108**, 12605 (2011).
[26] D. R. Daniels and M. S. Turner, Langmuir **23**, 6667 (2007).
[27] J. Howard, Annu. Rev. Biophys. **38**, 217 (2009).
[28] A. B. Kolomeisky and M. E. Fisher, Annu. Rev. Phys. Chem. **58**, 675 (2007).